JOURNAL OF MATERIALS SCIENCE 22 (1987) 3095–3102

Banding structures in induced morphology crystal aggregates of $CaCO_3$

S. DOMINGUEZ BELLA, J. M. GARCIA-RUIZ
Departamento de Geología, Facultad de Ciencias, Universidad de Cadiz, Apdo. 40, Puerto Real (Cádiz), Spain

Average radial growth rates in induced morphology crystal aggregates (IMCA) of $CaCO_3$ with sheaf-of-wheat morphologies range between 33.4 and 111 μm/day. The growth process has not been found to be diffusion-controlled. Banding structures appearing in this kind of IMCA are explained just like rhythmic structures similar in origin to Liesegang rings, but the banding law in this case being modified by the matrix effect. Genetical models explaining the formation of ribbons with different particle density are also proposed.

1. Introduction

Induced morphology crystal aggregates (IMCA) have been defined as composites with self-organized non-crystallographic morphologies [1]. They are formed by a cooperative growth of a silicated matrix and a crystalline phase (in this case, calcite ($CaCO_3$)) which acts as a catalyser.

In a previous paper [2] on the textural arrangements in IMCA of $CaCO_3$ with sheaf-of-wheat morphologies, the authors have found different kinds of banding structures. The aim of this paper is to present a kinetic and morphological study on the formation of such self-organized structures and to propose genetical models for them.

2. Experimental procedure

Induced morphology crystal aggregates of $CaCO_3$ were obtained by the reaction between $CaCl_2$ (0.5 M) and Na_2CO_3 (0.5 M) aqueous solutions at room temperature in a silica gel at pH 10. The device used was a U-shaped cassette, described elsewhere [2]. A sodium metasilicate solution (s.p. = 1.06 gm cm^{-3} and pH 11.2), acidified with HCl (N) up to the desired pH, was placed in the horizontal part of the cassette, and once gelled, the reacting solutions were poured into each branch so that counter-diffusion through the gel occurs.

As described in previous papers [1, 3], after a few hours a precipitation zone was observed in the gel. This zone is formed by a set of crystal aggregates of $CaCO_3$ associated to a silicated matrix showing different morphologies evolving as they grew. Radial growth rates of the aggregates were measured by time lapse microphotography, using an Olympus BH-2 microscope associated to a time controller.

The crystal aggregates were recovered from the gel by mechanical manipulation and dissolution with NaOH. After washing in doubly-distilled water and ethanol, and once dried, they were glued onto an aluminium base using double-faced adhesive tape. For scanning electron microscopy studies, these bases were coated with gold.

3. Results and discussion

The most suitable IMCA for a kinetic study are those showing non-crystallographic branching. They present a sheaf-of-wheat morphology. As shown in Fig. 1, when these aggregates form in the interface between the gel and glass walls of the cassette, their growth is restricted to two dimensions and then shows a double fan-like morphology. Thus, by time-lapse microphotography it is possible to measure with accuracy the radial growth rate of the aggregate.

The growth measurements were carried out on seven different crystal aggregates with the described morphology. All these aggregates were grown under identical initial conditions but they belong to different positions within the glass cassette and therefore have different chemical environments. Growth data are displayed in Table I. Fig. 2 shows six different growth stages belonging to a representative sequence (labelled A in Table I) of 15 photomicrographs with a time lapse of 24 h. Fig. 3 is a diagram of the overall A sequence showing the morphology and the successive growth period. The average radial growth rates found range between 33.4 and 110 μm/day. Crystal growth in porous media has been often described as a diffusion-controlled process. Consequently, a linear relation-

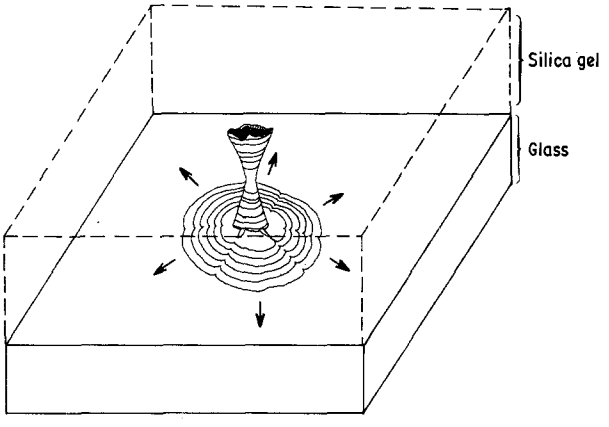

Figure 1 Sheaf-of-wheat aggregate grown on the gel/glass interface. Arrows show growth development on this interface.

0022–2461/87 $03.00 + .12 © *1987 Chapman and Hall Ltd.*

TABLE I Growth data of six IMCA aggregates grown in Silica Gels and a calcite rhombohedra grown in TMS gel

Sequence	l/t Linear correlation coefficient	l^2/t Linear correlation coefficient	Average growth rate (μm/day)	Morphology		Emplacement	
A	0.998	0.995	39	Sheaf-of-wheat aggreg.	with banding	Glass/gel interface	Silica gel
B	0.999	0.987	51.9	Sheaf-of-wheat aggreg.	with banding	Glass/gel interface	Silica gel
C	0.999	0.992	43.5	Sheaf-of-wheat aggreg.	with banding	Glass/gel interface	Silica gel
D	0.997	0.992	40.5	Sheaf-of-wheat aggreg.	with banding	Glass/gel interface	Silica gel
E	0.985	0.956	33.4	Sheaf-of-wheat aggreg.	with banding	Glass/gel interface	Silica gel
F	0.987	0.990	110	Sheaf-of-wheat aggreg. without banding		Glass/gel interface	Silica gel
G	0.966	0.988	4.7 ($l/2$)	Rhombohedra $\{1\,0\,\bar{1}\,1\}$ ([0 0 0 1] direction)		T.M.S. gel	

ship between the size of the crystal (l) and the square root of the time has been recorded many times. In fact, for the particular case of $CaCO_3$ (calcite) crystals growing in chemically inert gels (such as tetramethoxysilane), the present authors have found that the advance of the rhombohedral face $r[1\,0\,\bar{1}\,1]$ follows the equation:

$$r[1\,0\,\bar{1}\,1] = 45.36t^{1/2} + 215 \quad (1)$$

with a correlation coefficient of 0.9886.

However, for IMCA, a better fitting of the data to linearity is obtained in some cases when the radius of the crystal aggregate is plotted against time (Table I). That means that the growth rate of the composite is not exclusively governed by the transport from the bulk solution to the crystal surface, implying an important role of the coprecipitating membraneous matrix, so that the higher the amount of silicate matrix in the crystal aggregate, the greater the deviation of the kinetics of the process from the diffusion-controlled conditions.

We have elsewhere described the existence of two kinds of crystal aggregates [2]. One of them presents clear banding and will be studied in this paper. In Fig. 2, the existence of banding can be clearly observed. SEM views (Fig. 4) reveal that this structure

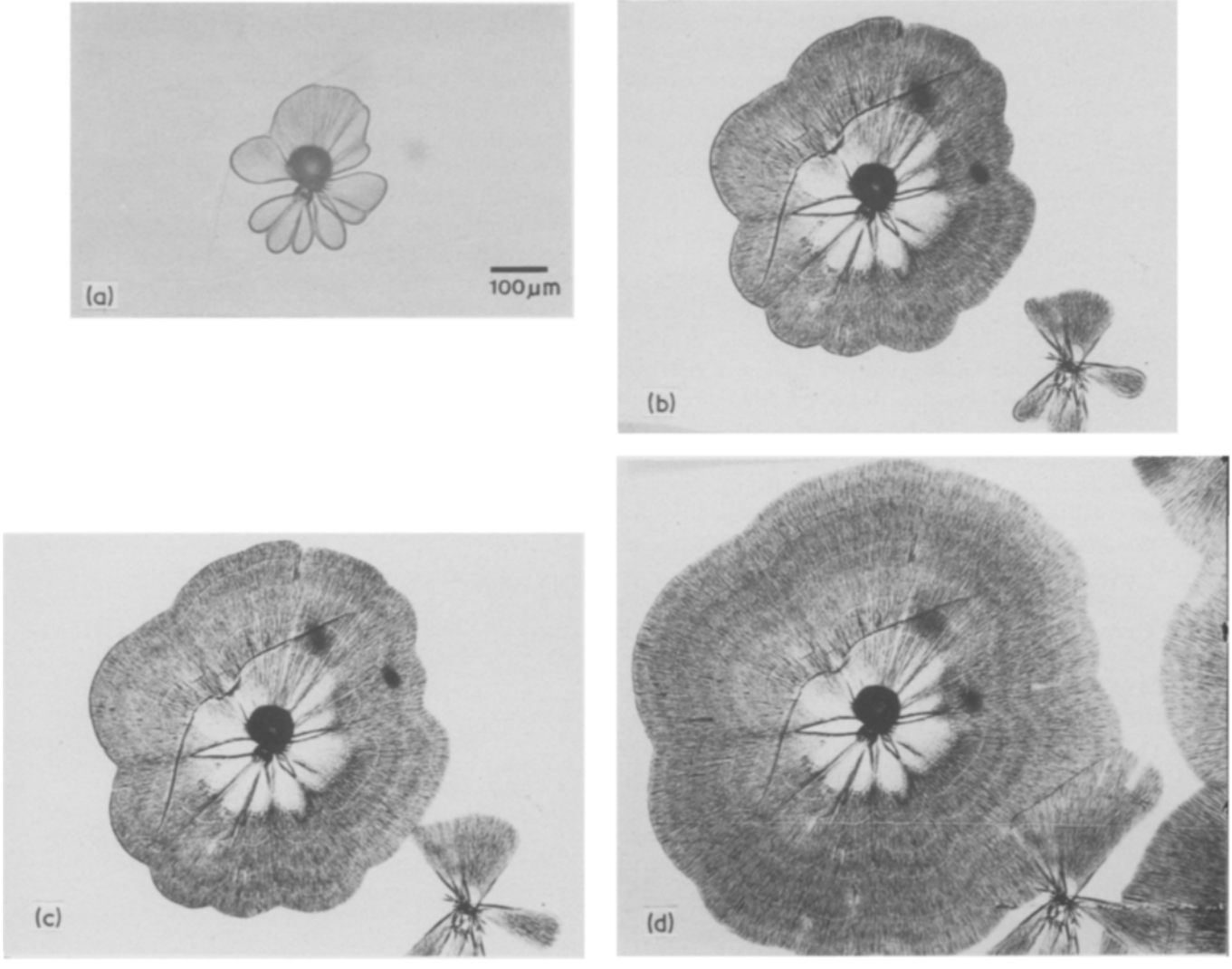

Figure 2 Optical views of six different growth stages of the aggregate of sequence A, at different times. (a) = 0 days; (b) = 3 days; (c) = 5 days; (d) = 7 days; (e) = 10 days; (f) = 19 days. (s.b. = sharp band).

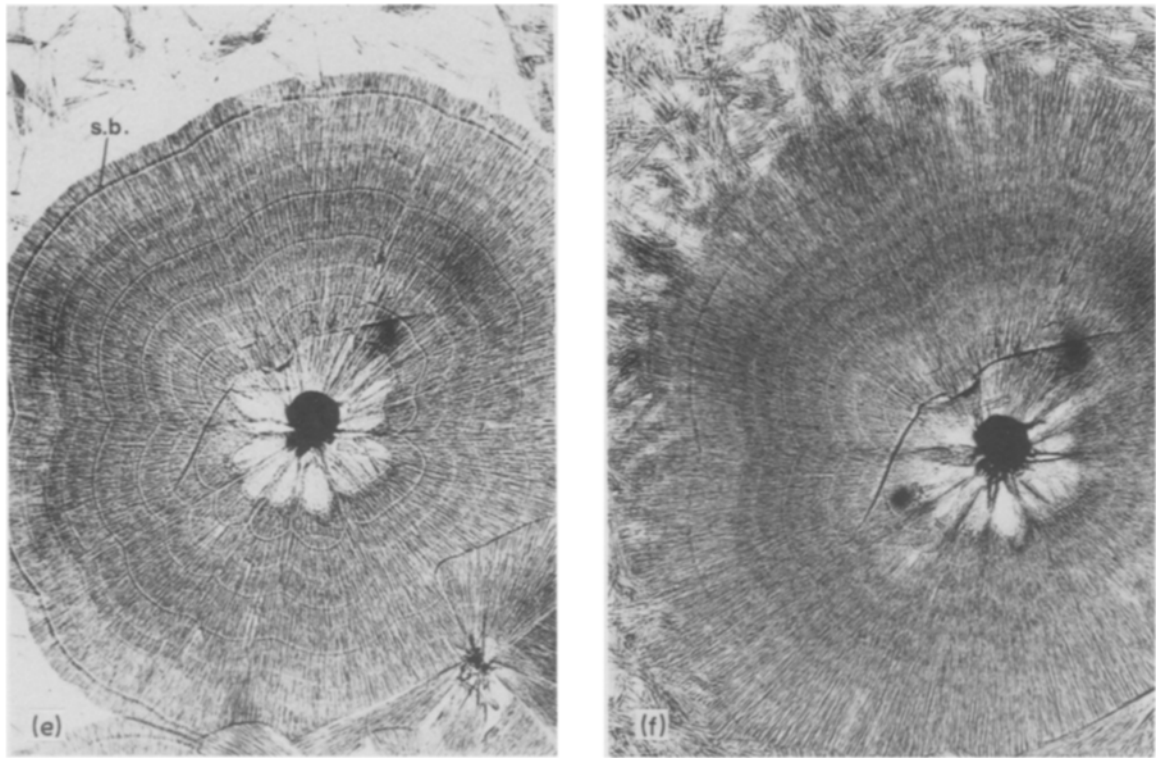

Figure 2 Continued.

consists of thick bands formed by enlarged calcite crystallites, arranged along the radius of the aggregates. These bands leave ribbons of low particle density between them. Although in some cases the outer bands are usually wider than those near the core, there are no banding patterns following single relationships (Fig. 5). In particular, neither linear nor Liesegang patterns [4] have been usually found, which agrees with the kinetics of the growth process. The sheaf-of-wheat aggregate itself is built by micro sheaves of

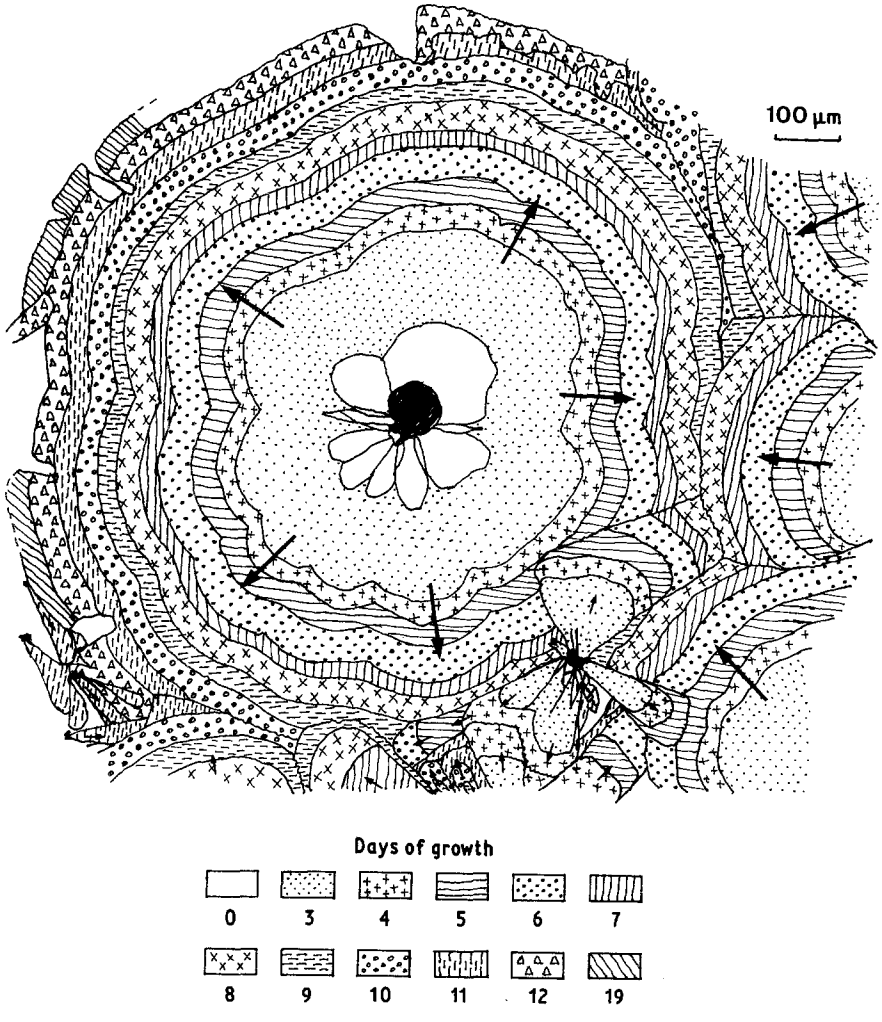

Figure 3 Diagramatic model of growth on aggregate in sequence A. Time of sequence is shown. Arrows show growth directions.

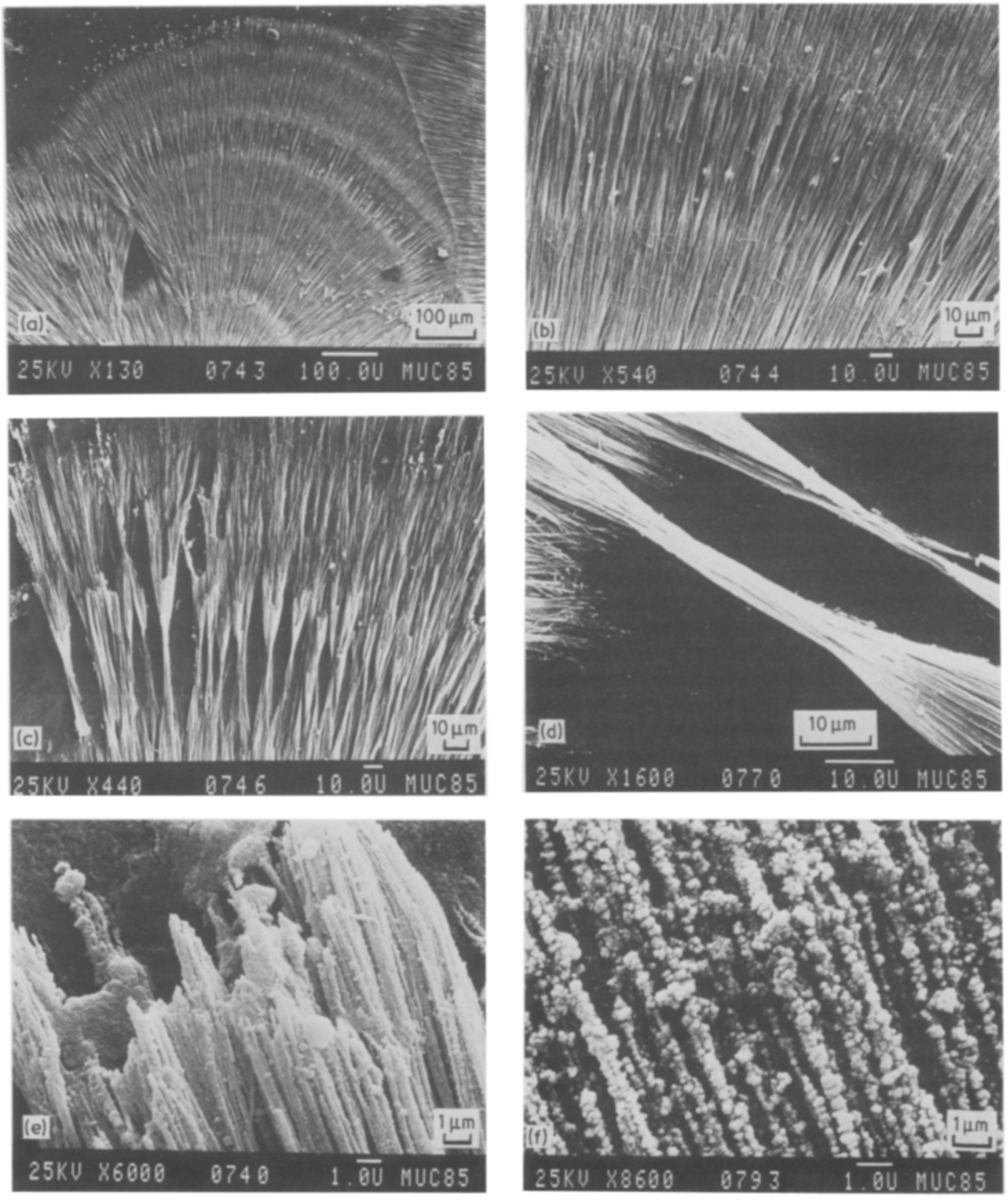

Figure 4 SEM views of different aspects in sheaf-of-wheat aggregates. (a) general view; (b) and (c) details of the banding; (d) micro-sheaf of wheat; (e) and (f) details of fibres.

wheat arranged along radial directions (Fig. 4d). Each fibre is made up of a set of calcite single crystal rhombohedra arranged along the *c*-axis |0 0 0 1| (Fig. 4e and f). The size of the different particles (rhombohedra, fibres and micro sheaves of wheat) is not a typical feature of the $CaCO_3$ IMCA.

SEM studies reveal that the existence of banding, i.e. concentric ribbons of high and low particle density, is related to the sheaf-of-wheat model. Thus, as shown in Fig. 6a low density zones belong to the geometrical locus of the points displayed by the centre of the micro-sheaves and high density zones to those displayed by its two symmetrical fans. In some cases, optical micrographs show sharp black bands belonging to ribbons with very large particle size (s.b. in Fig. 2e). In fact, SEM microscopy shows that these bands are formed by large single crystals of calcite with clear rhombohedron morphology (Fig. 6b). Even in these cases the orientation of the crystals is along |0 0 0 1|.

Our results clearly show that the existence of banding is a phenomenon completely independent of day–night process or other periodicity external to the system. Bands are also formed in experiments carried

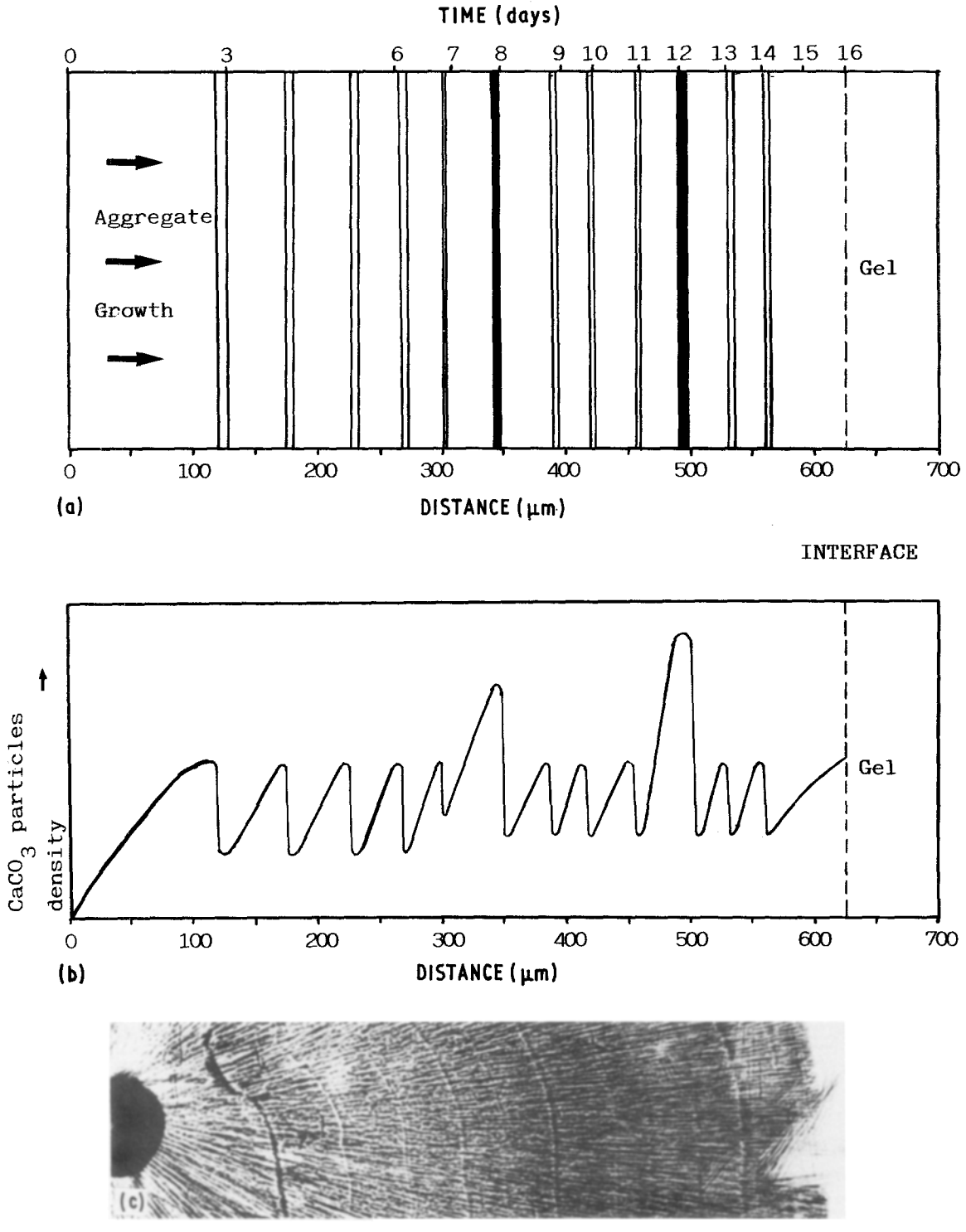

Figure 5 (a) Banding emplacement along the radius of Fig. 2 aggregate, from the centre of this to the interface gel/aggregate. (b) Diagramatic representation of $CaCO_3$ particle density along this radius. (c) Optical view of the banding.

out in darkness. Therefore the banding structure should be explained as a self-organized structure related to the very growth process. The existence of rhythmic crystallization or banding can be explained by the Mullins–Sekerka theory [5], which establishes that wavelength fluctuations greater than a critical value grow deforming the planar front, this critical value being a decreasing function of the growth rate. There is a change in the degree of supersaturation in the normal to the advancing front solution. This change can be explained as a result of the rate of evolution of latent heat (which depends on the thermal diffusivity of the solution) or by considering the patterns of concentration and the diffusion of the solute at the interface (i.e., the break of the steady state in the normal to the front). The first process has been used to develop a qualitative model for the rhythmic crystallization of evaporating thin films of ascorbic acid solutions [6]. Williamson [7] also uses the concept of constitutional supersaturation (the analogue of constitutional supercooling for solution growth) for the case of Portland cement, a material chemically similar to the IMCA crystal aggregates. However, the phases forming these crystal aggregates, calcium silicate hydrate and calcium carbonate, are both poorly soluble and also weakly sensitive to temperature.

For the more soluble phase, $CaCO_3$, Garrels and

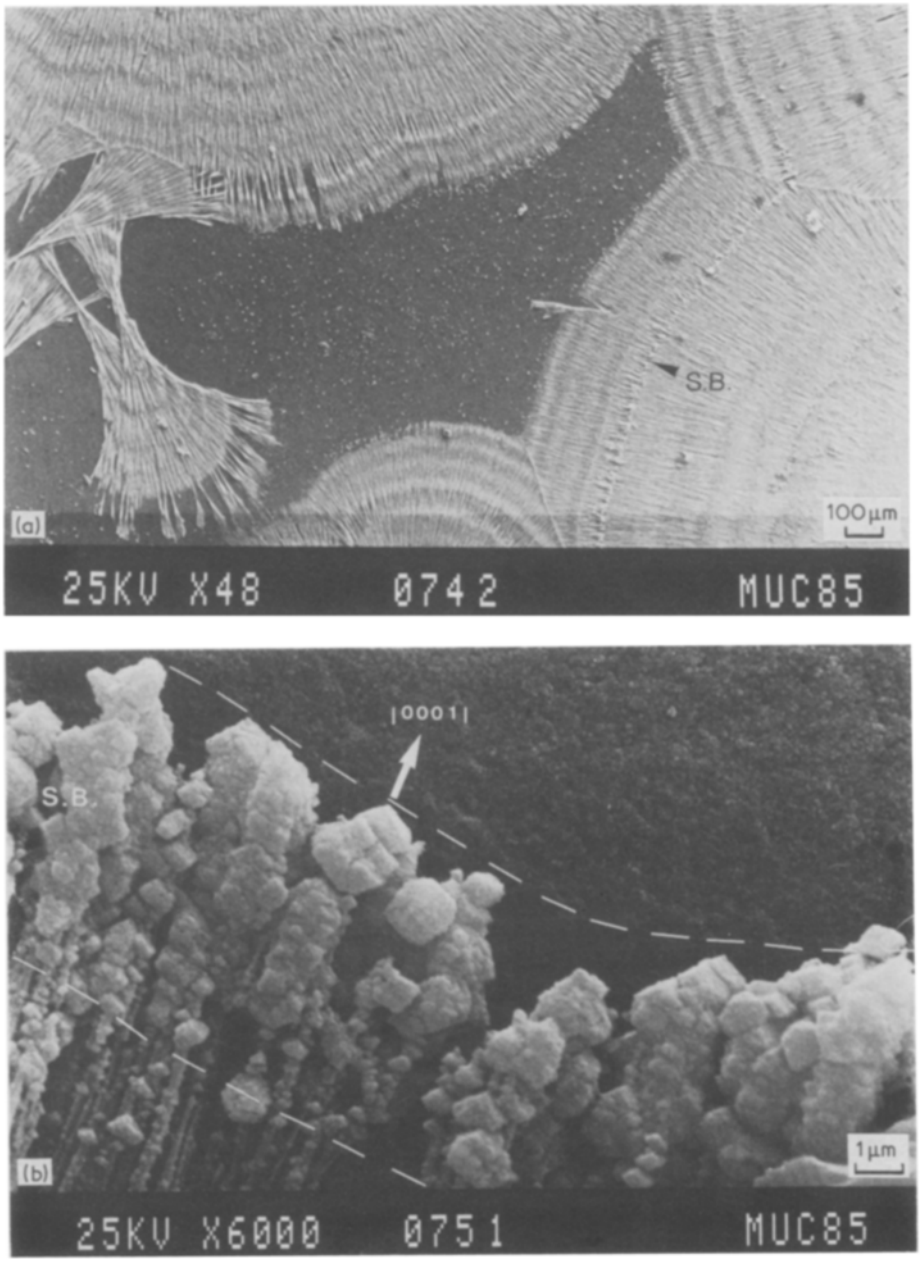

Figure 6 (a) SEM view of several sheaf-of-wheat aggregates. (b) Detail of a sharp band (s.b.), in the growth front of an aggregate. The rhombohedral crystals arrangement along their |0001| axis can be seen.

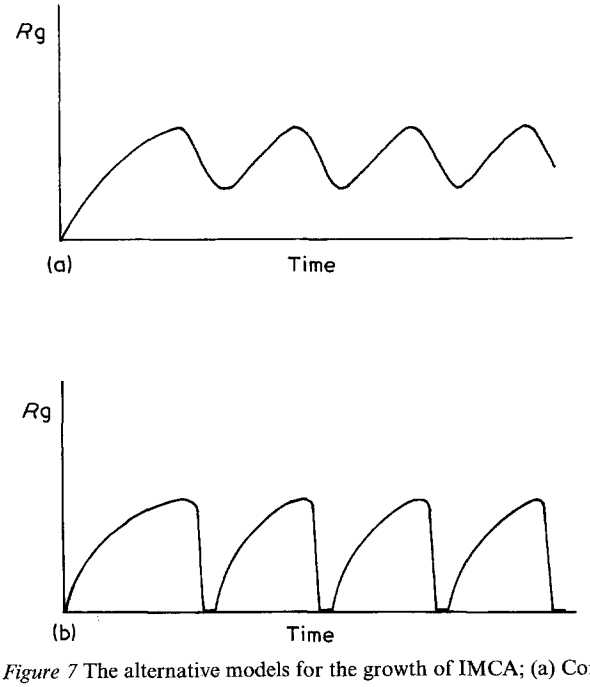

Figure 7 The alternative models for the growth of IMCA; (a) Continuous growth (b) Nucleation + Growth.

Christ [8] give the variation of concentration as a function of the temperature. By using these data, it can be demonstrated that the absolute supersaturation obtained after assuming a temperature gradient of 60° C is 4.01×10^{-5} mol l^{-1}. After these values, it is very difficult to justify the existence of a periodical precipitation as a result of the compromise between the amount of substance consumed during the growth process and that diffusing from the bulk solution to the precipitation front, i.e. just like a rhythmic structure similar in origin to Liesegang rings [9].

It is interesting to know if the formation of IMCA is a continuous process, i.e., if the growth rate is always positive and the banding structure appears as a change in the number and size of the crystals, or on the other hand, if there is at least one instant at which the growth rate is zero, and therefore, successive stages of nucleation and growth occur (Fig. 7). In order to check this, the time lapse, $t1$, used in the photomicrographic series ($t1 = 24$ h) was too great and consequently each picture presented a new band. From these data it was impossible to establish the

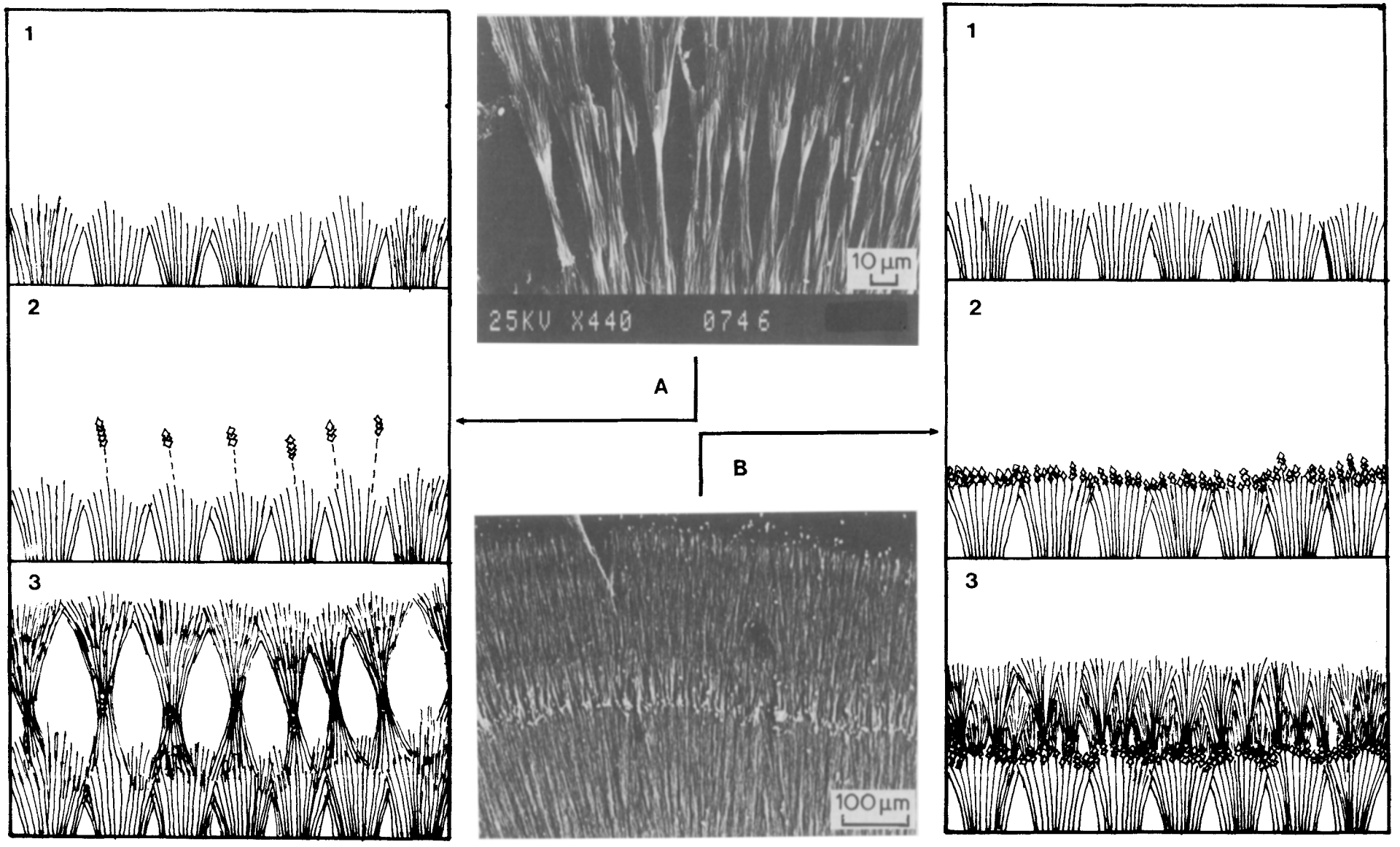

Figure 8 Diagrammatic models of banding formation in sheaf-of-wheat aggregates. A, Low density bands; B, high density bands (s.b.).

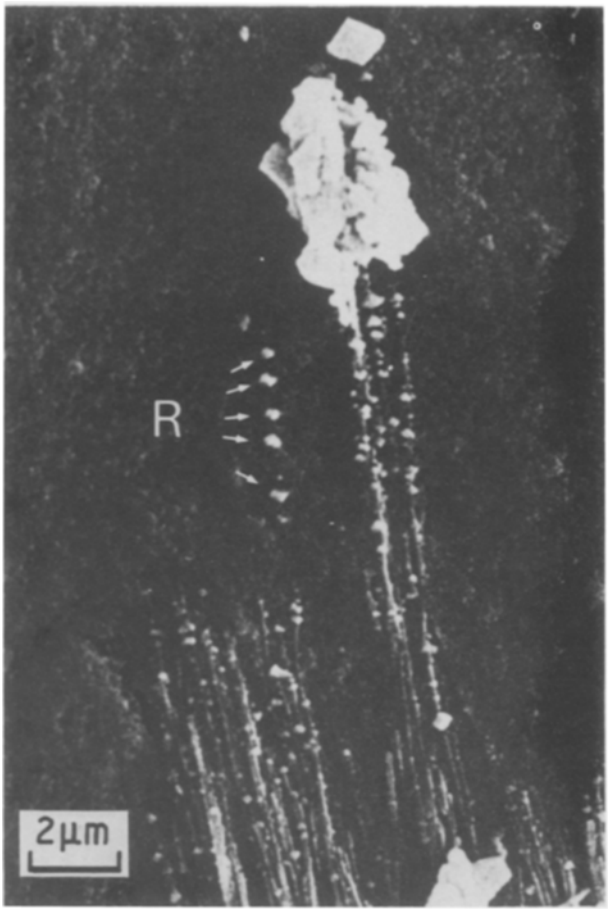

Figure 9 SEM view of growth front in a sheaf-of-wheat aggregate. (R): Rhombohedral crystals arranged along |0001| axis and the axis-fibre, without physical contact between them.

character of the growth process. However, observing growth fronts under SEM, isolated calcite single crystals, R, can be seen at some microns from the interface, without physical contact between them, supporting the nucleation and growth hypothesis. On the other hand, the fact that those crystallites are well orientated in relation to the aggregate, supports the idea that there is a connection via matrix between them and the aggregate which has not been detected by SEM (Fig. 9).

Whether the nucleation of calcite rhombohedra is homogeneous or controlled by silicated matrix, these processes give well-defined banding models as shown in Fig. 8a. These models explain the formation of low density bands that can be observed in sheaf-of-wheat morphologies found in $CaCO_3$ IMCA.

However, in other cases, the nucleation has been found to be clearly controlled by the matrix. These rhombohedra crystals are nucleated just on the outer fans of the micro-sheaves that form the interface between the IMCA and the gel. These rhombohedra will be the cores of the micro-sheaves forming the next band. Thus, as diagrammatically shown in Fig. 8b, this model explains the high density (s.b.) found in sheaf-of-wheat IMCA of $CaCO_3$.

4. Conclusions

A genetical model of banding formation in $CaCO_3$ IMCA is proposed, based on the compromise between the amount of matter absorbed during the growth of the aggregate and that diffusing from the solution to the aggregate's growth front. This process shows an ondulatory behaviour, in which in some cases, successive stages of nucleation and growth occur.

The growth rates recorded are higher than those found in single crystals of $CaCO_3$ grown in tetramethoxysilane (TMS) gels, suggested a catalytic effect of the silicated matrix on the nucleation and growth of the carbonated crystals and therefore on the formation of the whole aggregate.

Acknowledgements

The authors wish to thank Dr J. M. Gomez de Salazar of the Department of Metallurgy (Universidad Complutense de Madrid) for his collaboration in the SEM study, and Ms P. Peers for editorial assistance. This work has been supported by the SEUI project.

References

1. J. M. GARCIA-RUIZ, *J. Crystal Growth* **73** (1985) 251.
2. S. DOMINGUEZ BELLA and J. M. GARCIA-RUIZ, *ibid.* **79** (1986) 236.
3. J. M. GARCIA-RUIZ and J. L. AMOROS, *ibid.* **55** (1981) 379.
4. R. E. LIESEGANG, "Chemische Reaktionen in Gallerten" (Verlgtheodor Steinleopf, Dresden, 1924).
5. W. W. MULLINS and R. F. SEKERKA, *J. Appl. Phys.* **35** (1964) 444.
6. K. IWAMOTO, S. MITOMO and M. SENO, *J. Coll. Interface Science* **102** (1984) 477.
7. R. B. WILLIAMSON, *J. Crystal Growth* **3/4** (1968) 787.
8. R. M. GARRELS and C. L. CHRIST, "Solutions, Minerals and Equilibria" (Harper & Row, New York, 1965).
9. H. K. HENISCH and J. M. GARCIA-RUIZ, *J. Crystal Growth* **75** (1986) 195.

Received 13 October 1986
and accepted 22 January 1987